

Report 2181

660 TC 94V



DEPARTMENT OF THE NAVY

SUMMARY REPORT OF WIND-TUNNEL INVESTIGATIONS OF A 1/20-  
SCALE POWERED MODEL OPEN-OCEAN V/STOL SEAPLANE

by

Richard O. Thomas

HYDROMECHANICS

○

AERODYNAMICS

○

STRUCTURAL  
MECHANICS

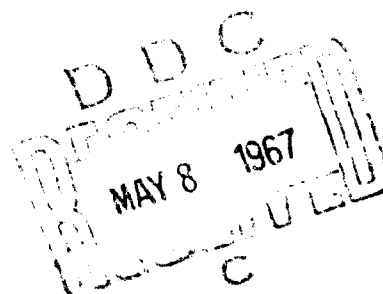
○

APPLIED  
MATHEMATICS

○

ACOUSTICS AND  
VIBRATION

Distribution of this document is unlimited.



AERODYNAMICS LABORATORY  
RESEARCH AND DEVELOPMENT REPORT

ARCHIVE COPY

January 1967

Report 2181

SUMMARY REPORT OF WIND-TUNNEL INVESTIGATIONS OF A 1/20-  
SCALE POWERED MODEL OPEN-OCEAN V/STOL SEAPLANE

by

Richard O. Thomas

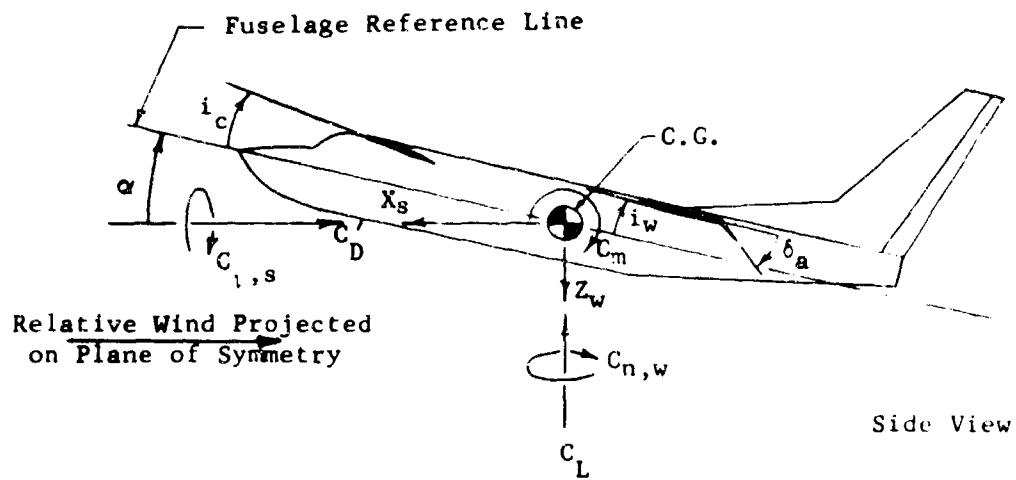
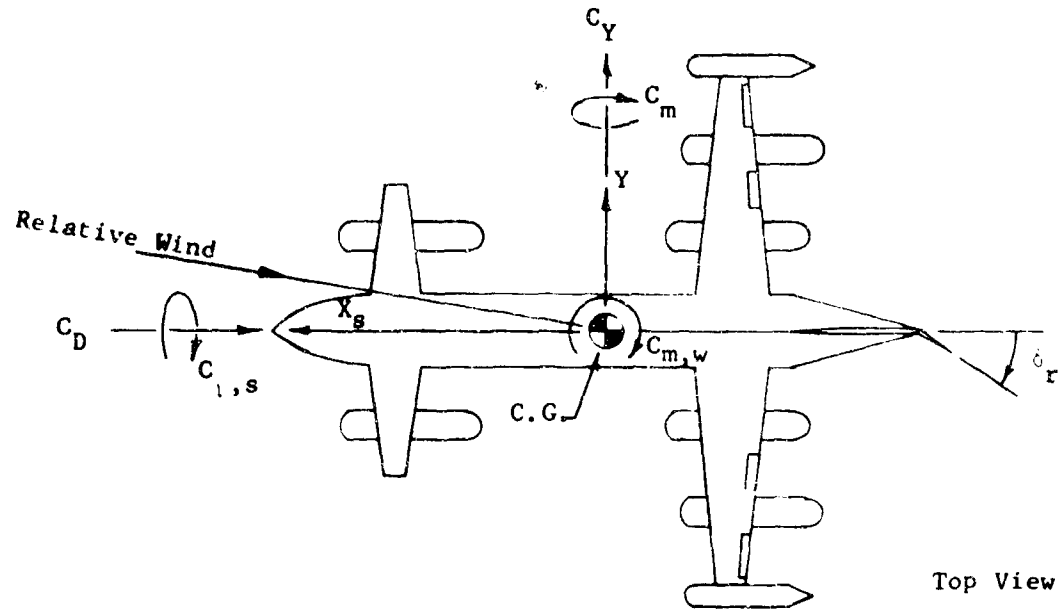
Distribution of this document is unlimited.

January 1967

Report 2181  
Aero Report 1106

# NOTATION

Positive directions of axes, forces, moments, and angular displacements are shown by arrows.



Axis	Force in pounds	Force Coefficient	Moment in pound-feet	Moment Coefficient
$X_s$	$F_D$	$C_D' = F_D'/qS$	$M_{Xs}$	$C_{l,s} = M_{Xs}/qSb_w$
$Y$	$F_Y$	$C_Y = F_Y/qS$	$M_Y$	$C_m = M_Y/qS\bar{l}$
$Z_w$	$F_L$	$C_L = F_L/qS$	$M_{Zw}$	$C_{n,w} = M_{Zw}/qSb_w$

# SYMBOLS

b	span in feet
c	local chord in feet
$\bar{c}$	mean geometric chord in feet
$l$	distance between hinge lines of wings in feet
P	power in foot-pounds per second
q	dynamic pressure $\left(\frac{\rho V^2}{2}\right)$ in pounds per square foot
R	Reynolds number per foot $\left(\frac{\rho V}{\mu}\right)$
S	total of wing and canard areas in square feet
$S_m$	momentum area $\left(\frac{\pi b_w^2}{4}\right)$ in square feet
V	airspeed in feet per second
W	airplane weight in pounds
L	lift force in pounds
P	nondimensional power parameter $\left(\frac{P}{L \sqrt{\frac{L}{\rho S_m}}}\right)$
v	nondimensional speed parameter $\sqrt{\frac{2}{C_{L_m}}} = \sqrt{\frac{2q S_m}{L}}$
$\rho$	density of air in slugs per cubic foot
$\mu$	absolute coefficient of viscosity in pound-second per square foot

## Angular Settings

$\alpha$	angle of attack in degrees (angle between fuselage reference line and the projection of the relative wind vector on the plane of symmetry of the aircraft)
$\beta$	angle of sideslip in degree (angle between relative wind vector and plane of symmetry of aircraft)

#### SYMBOLS (Concluded)

- $i_c$  angle of forward wing in degrees (angle between fuselage reference line and root chord line of forward wing)
- $i_w$  angle of rear wing in degrees (angle between fuselage reference line and root chord line of rear wing)

#### Subscripts

- c forward wing (canard)
- w rear wing

## TABLE OF CONTENTS

	Page
NOTATION	ii
SYMBOLS	iii-iv
SUMMARY	1
INTRODUCTION	1
MODEL AND APPARATUS	2
TEST CONDITIONS AND PROCEDURES	3
RESULTS	3
DISCUSSION	6
CRUISE PERFORMANCE	6
TRANSITION TESTS	8
REFERENCES	10

## LIST OF TABLES

Table 1 - Geometric and Physical Characteristics of a 1/20-Scale Powered Model Open-Ocean V/STOL Seaplane	11-12
Table 2 - Summary of Wind Tunnel Test Conditions for a 1/20-Scale Powered Model V/STOL Seaplane in the Transition Configuration	13

## LIST OF ILLUSTRATIONS

Figure 1 - Principal Dimensions of a 1/20-Scale Tilt-Wing V/STOL Seaplane Model	14-15
Figure 2 - Propeller Rotation Directions for a 1/20-Scale Powered Model V/STOL Seaplane	16
Figure 3 - Photographs of the Seaplane Model in the Wind Tunnel	17-19
Figure 4 - Dimensions of Full-Span Spoilers for Wing and Canard of 1/20-Scale V/STOL Seaplane Model	20
Figure 5 - Effect of Reynolds Number Correction to Minimum Drag and $C_{L_{max}}$ on Aerodynamic Characteristics of Open-Ocean V/STOL Seaplane	21-23
Figure 6 - Power Required Parameter as Measured in the Wind Tunnel and Calculated From Power-Off Wind Tunnel Tests	24
Figure 7 - Performance Comparison of the Seaplane With a Monoplane of Equivalent Size and Aspect Ratio	25-28
Figure 8 - Horsepower Required Versus Speed for a Full-Scale Seaplane. Sea Level; Standard Day; Weight = 93,000 Pounds	29

TABLE OF CONTENTS (Concluded)  
LIST OF ILLUSTRATIONS (Concluded)

	Page
Figure 9 - Longitudinal Aerodynamic Characteristics in Pitch at Various Wing Tilts for a 1/20-Scale Model V/STOL Seaplane. Thrust Set for $C_D = 0$ at $\alpha = 0^\circ$	30-31
Figure 10 - Lateral-Directional Aerodynamic Characteristics in Sideslip at Various Wing Tilts for a 1/20-Scale Model V/STOL Seaplane. Thrust Set for $C_D = 0$ at $\alpha = 0^\circ$	32-34
Figure 11 - Wing Tilt Versus Airspeed for Various Climb and Sink Angles. Fuselage Level; Spoilers Off; Weight = 93,000 Pounds; Sea Level, Standard Day	35
Figure 12 - Effect of Full-Span Spoilers on Powered Required	36
Figure 13 - Static Longitudinal Stability Versus Wing Tilt	37

## SUMMARY

Low-speed wind-tunnel tests were conducted on a 1/20-scale powered model of a proposed open-ocean V/STOL seaplane design. Hover and transition power required and climb and descent speeds at various flight path angles were determined. The effect of full-span spoilers on wing and canard stalling characteristics through transition was briefly investigated.

A comparison of cruise performance of the seaplane and a conventional transport of equivalent size was made. After correction of the seaplane model cruise lift curve and drag polar to full-scale Reynolds number, cruise performance of the seaplane was found to compare favorably with that of the conventional monoplane.

In the transition mode, the model is longitudinally unstable at high wing tilts and directionally stable at all wing tilts for the initial center-of-gravity location. With the present relationship of wing, canard, and center of gravity, the model cannot be trimmed in pitch by varying only incidence of the canard with uniform thrust setting on all engines. Differential thrust, the mechanism envisioned for hover control, is necessary for pitch trim and control throughout most of the transition mode.

## INTRODUCTION

A low-speed wind-tunnel investigation of a 1/20-scale powered model of the Open-Ocean V/STOL Seaplane was conducted to determine the power required and longitudinal and lateral-directional stability for hover and transition flight, and STOL speeds. The variable parameters included pitch, yaw, wing tilt, and thrust coefficients. The seaplane design is the result of a study at the Aerodynamics Laboratory to investigate the feasibility of combining high payload-range capability in cruise and V/STOL characteristics in the same aircraft. The six-engine tilt-wing seaplane is a canard configuration employing a large wing with four propellers at the rear of the fuselage and a smaller canard lifting surface with two propellers near the nose. Its primary mission would be antisubmarine warfare. The design considerations

of the V/STOL seaplane are more fully described in Reference 1, which presents the aerodynamic characteristics of the model in the cruise configuration.

The transition tests were conducted during the period 11 March 1965 to 5 April 1965 in the 17- by 20-foot low-speed test section of the TMB Subsonic Wind Tunnel 2.

Although some cruise data were presented in Reference 1, a further analysis and comparison of the cruise data with that of a conventional airplane configuration is presented. This report completes the presentation of results of the seaplane model wind-tunnel tests.

#### MODEL AND APPARATUS

The 1/20-scale model is constructed of mahogany with internal metal wing spars. The wing and canard are covered with a fiberglass skin to provide additional strength. Principal dimensions of the model are shown in Figure 1, and the model geometric and physical characteristics are given in Table 1. The area of the vertical tail was reduced by 28 percent after the tests of Reference 1 showed that the seaplane was too stiff directionally in cruise flight.

The wing and canard are hinged on the model fuselage as shown in Figure 1, and each surface may be tilted through an incidence range of  $0^\circ$  to  $90^\circ$  by its own linear actuator and mechanical linkage.

The model motors are housed in larger-than-scale nacelles on the wing and canard. The difference in size between scaled nacelles and the model motor nacelles is shown in Figure 1.

Model power is provided by a 13.5- $\phi$  variable-frequency electric motor in each nacelle driving a scaled, four-bladed fiberglass propeller. Propeller rotation is as shown in Figure 2.

Two types of propellers were used. Conventional twisted cruise propellers were mounted on the two inboard nacelles on the wing, while untwisted, high-solidity hover propellers were mounted on the four remaining nacelles.

The model was supported on a single strut and pitched by a linear actuator in the fuselage. Angles of sideslip were obtained by rotating the single strut. Photographs of the model mounted in the wind tunnel are shown in Figure 3.

### TEST CONDITIONS AND PROCEDURES

The transition tests were conducted in the 17- by 20-foot low-speed section of the TMB Subsonic Wind Tunnel 2 for the conditions given in Table 2. Propeller blade angles, rpm, and wind speed were selected such that drag on the model was zero at  $\alpha = 0^\circ$  for the basic runs. For determination of climb and descent speeds, the drag or thrust corresponding to climb or sink angles of  $5^\circ$  and  $10^\circ$  was set by varying the wind speed.

No control surface deflections were tested, the control surfaces being set at  $0^\circ$  with sealed gaps throughout the test.

An attempt was made to trim the model in pitch by varying incidence of the canard. However, this is not a completely effective means of trimming pitch, and thus all runs were made with the wing and canard incidences the same and with the model out of trim.

Full-span spoilers of the type shown in Figure 4 were attached to the wing and canard at the 15 percent chord line. The same thrust was set on the model as was used for trimmed drag runs without spoilers.

Test conditions and procedures for the cruise configuration data are outlined in Reference 1.

### RESULTS

Aerodynamic characteristics of the seaplane model are presented graphically in coefficient form. The aerodynamic force and moment coefficients, and the axis system to which they are referred, are defined in the notation. Model constants used in computing coefficients are as follows:

$$S = 3.125 \text{ square feet}$$

$$S_m = 19.635 \text{ square feet}$$

$$b_w = 5.0 \text{ feet}$$

$$l = 2.614 \text{ feet}$$

Tare and interference effects of the single-strut support were considered negligible at the low tunnel test speeds used in the 17- by 20-foot test section. No jet-boundary corrections were made, as these were also found to be negligible for the 17- by 20-foot section, when computed by Heyson's method (Reference 2).

All coefficients are based on free-stream dynamic pressure rather than the more conventional  $q''$  (free-stream dynamic pressure plus propeller disc loading), since true propeller shaft thrust is not known.

The model propellers were calibrated singly in the 8- by 10-foot test section of the TMB Subsonic Wind Tunnel 1. This calibration is not valid for the 17- by 20-foot test section, mainly because of the wall-induced difference in inflow angles between test sections at high propeller plane pitch angles. A propeller calibration in the 17- by 20-foot test section was not made, owing to lack of time. However, the model power measurement was considered to be relatively accurate for the very high wing-tilt, low-speed condition in the 17- by 20-foot section and for the cruise conditions of the 8- by 10-foot section tests. Wall-induced changes of inflow angle are small for these conditions.

The nondimensional power-required parameter  $\bar{P}$  and speed parameter  $\bar{v}$  presented are defined as follows:

$$\bar{P} = \frac{P}{L \sqrt{\frac{L}{\rho S_m}}}$$

$$\bar{v} = \sqrt{\frac{2}{C_{L_m}}}$$

Full-scale values of horsepower and speed may be found by dimensionalizing these parameters using airplane weight and the pertinent atmospheric conditions.

Constants used in computing power and speed parameters, full-scale horsepower required, and STOL speeds are:

$$S_m = \begin{array}{l} 7,854 \text{ square feet, full scale;} \\ 19 \text{ square feet,} \\ \text{model scale} \end{array}$$

$$W = 93,000 \text{ pounds}$$

$$\rho = 0.00238 \text{ slug per cubic foot (standard sea-level atmosphere)}$$

In order to compare the performance of the model seaplane with that of conventional airplanes, corrections to cruise maximum lift coefficient and minimum drag coefficient were made. The drag polar was shifted to account for lower parasite drag of a full-scale vehicle flying at much higher Reynolds number than that at which the model was tested. The lift curve was extended to account for an expected increase in  $C_{L_{max}}$  for a full-scale vehicle. These corrections were made in accordance with procedures outlined in References 3, 4, and 5. The effect on the seaplane cruise lift curve, drag polar, and lift-drag ratio is illustrated in Figure 5.

Power required parameter versus speed parameter is presented in Figure 6. The power-off curve was obtained from the power-off drag polar, corrected for Reynolds number. A propeller efficiency of 0.7 was assumed in this calculation. The power-on curve was measured directly in the wind tunnel and not corrected for Reynolds number, since a correction of this type, in this low-speed range, is meaningless. The power required to hover ( $v = 0$ ) was calculated because model hover tests showed unrealistically high power required. The restriction and recirculation of airflow imposed by the wind-tunnel walls undoubtedly gave erroneous model power measurements in hover. The two curves in Figure 6 were faired together to obtain the seaplane power-required curves illustrated in Figures 7 and 8.

Figure 7 presents a comparison of the seaplane with a conventional monoplane of  $A = 8$  (the same aspect ratio as the seaplane, based on total wing area). This fictitious monoplane has the same span, wing area, and weight as the seaplane. Drag data for this airplane were estimated using methods outlined in Reference 4 and the assumption of a parabolic drag polar. This fictitious monoplane is a four-engine turbo-prop transport. A propeller efficiency of 0.7, the same as the seaplane, was assumed.

Full-scale horsepower required versus speed is presented in Figure 8 for the seaplane at sea level on a standard day at its VTOL weight of 93,000 pounds. Figures 9 and 10 present typical aerodynamic characteristics of the seaplane as measured in the wind tunnel. Wing tilt versus

full-scale speed for various climb and sink angles is presented in Figure 11. Figure 12 shows the effect of the full-span spoilers, illustrated in Figure 4, on power required in transition. This Figure also shows wing tilt required at various speeds, spoilers on and off. Figure 13 presents static longitudinal stability of the seaplane model in the transition mode.

## DISCUSSION

### CRUISE PERFORMANCE

It was stated in Reference 1 that the maximum measured lift-drag ratio for the seaplane was much lower than desired. In an effort to obtain a more realistic value of  $(L/D)_{\max}$  for a full-scale seaplane, a Reynolds number correction to maximum lift coefficient and minimum drag coefficient was made. The methods used are outlined in References 3, 4, and 5. As shown in Figure 5, this correction resulted in a  $C_{L_{\max}}$  increase of 20 percent, a decrease of  $C_{D_{\min}}$  of about 20 percent, and an increase in  $(L/D)_{\max}$  of about 17 percent. This correction also resulted in  $(L/D)_{\max}$  occurring at a  $C_L$  of 0.66, the design  $C_L$  for cruise with fuselage level. This corrected  $(L/D)_{\max}$  of 13.6 now compares favorably with the original design estimate of 14.0.

Figure 6 presents power-required parameter versus speed parameter as obtained from measured power results of model transition tests and calculated from the corrected power-off drag curve of the cruise tests. A measured propeller efficiency in cruise of 0.7 was used in the computations. The point at hover ( $v = 0$ ) on the power-on transition test curve was calculated rather than measured, as explained previously. These two power curves were faired together to produce a power curve for the entire speed range. This faired curve is used as the seaplane power-required curve throughout the remainder of this report.

Figure 7 presents a cruise performance comparison of the seaplane with the equivalent monoplane. Incidence of the monoplane wing was set to give the same fuselage-level  $C_L$  as obtained on the seaplane. A propeller efficiency of 0.7 was also assumed for the monoplane. Drag

estimates were based on methods outlined in Reference 4. The seaplane has a steeper lift-curve slope than the monoplane, and a slightly lower value of  $C_{L_{max}}$ . The lower stall angle is undoubtedly due to stalling of the front wing, which should occur at a true angle of attack of  $16^\circ$  or a fuselage angle of attack of  $10^\circ$ , considering the  $6^\circ$  fixed incidence angle of the front wing. The rear wing stalls at a fuselage angle of attack of  $13^\circ$  or an effective angle of attack of  $16^\circ$  ( $i_w = 3^\circ$ ). Thus, the seaplane has a slightly higher stall speed and conventional flight-mode landing speed than a monoplane of equivalent size.

Figure 7b shows that at the design cruise  $C_L$  of 0.66, the drag values of the two aircraft are the same. The seaplane drag curve bends more sharply about its minimum drag point, and the polar is not parabolic.

The minimum drag point of the seaplane does not occur at  $C_L = 0$  because the minimum drag incidences of the front and rear wings are never reached simultaneously, due to the difference in wing incidence.

The distortion from a parabola of the seaplane drag polar is due partially to the effect of the downwash field of the forward wing on the rear wing lift, and partially to the fuselage and nacelles, which produce some induced drag at an angle of attack.

Outboard of the tips of the forward wing there is a strong upwash field due to the tip vortex, which will increase the lift on the outer halves of the rear wing, thus increasing induced drag. Inboard of the front wing tips the downwash of the forward wing will decrease the lift on the rear wing, thereby decreasing induced drag. It is not possible to say at this time which of these is the more powerful, but it is suspected that the upwash outboard of the forward wing tips may be dominant. Also, local flow separations on the rear wing induced by the wake of the forward wing and nacelles may be a large contributor to this drag rise. No drag buildup tests were performed, and thus it is impossible to say exactly how much of this drag rise is due to fuselage and nacelles and how much is due to the effect of the forward wing downwash on the lift of the rear wing. Note that the seaplane cruise drag polar was obtained using scale nacelles and not the oversize model motor nacelles.

Maximum lift-drag ratios for the seaplane and the conventional monoplane (Figure 7c) are about the same and occur close to the design cruise lift coefficient.

An examination of power required (Figure 7d) reveals that at design cruise speeds ( $v \approx 4.5$  to  $5.5$ ) the seaplane will require about the same power as the conventional monoplane. At high dash speeds, however, the seaplane will require somewhat more power and thus, more fuel. (At low speeds, the conventional monoplane will require less power; however, the seaplane is envisioned as a VTOL and STOL vehicle and a comparison in this area may be somewhat misleading.)

Summarizing the cruise performance comparison, the seaplane's cruise performance compares well with that of a transport-type conventional airplane of equivalent size and weight. Speaking only of the design cruise performance, there is little difference shown between the airplanes, as would be expected, due to the tradeoffs which have to be made to obtain satisfactory V/STOL performance. Since the seaplane has much more wetted area, more engines, and more interference drag, a conventional airplane has a large advantage in aerodynamic cleanness and therefore may have an edge in cruise performance.

A dimensionalized horsepower-required curve for the seaplane is presented in Figure 8.

#### TRANSITION TESTS

Typical aerodynamic data for the seaplane in the transition mode are presented in Figures 9 and 10. Speed for various climb and sink angles versus wing tilt are presented in Figure 11. This curve presents wing tilt required for a desired climb or sink angle and speed.

The effect of full-span spoilers on power required is illustrated in Figure 12. Full-span spoilers, as illustrated in Figure 4, were attached to both wings in an attempt to keep the airplane lift curve smooth through transition, and thereby eliminate the deficiencies in handling qualities associated with descent transition of tilt-wing aircraft. No problems of sudden wing stall in transition were evidenced by the total force measurements on the constrained model, with spoilers on or off; and no change in the shape of the curve of total model lift versus

wing tilt was noted. At moderate wing tilts with spoilers on, a large drag increase was present along with a decrease in lift, dictating higher power required and higher wing tilt required at a given speed. At very high wing tilts, the presence of the spoiler behind the propellers increased power required without changing wing tilt required significantly. In this range (very high tilt angle), spoilers on a flying aircraft would be retracted to reduce the hover power requirement. At the moderate tilt angles, the increased drag (greater power requirement) is held to be advantageous in solving the handling qualities problem. However, the drag rise noted is believed to be secondary in importance to an alteration of the lift, which was not evident in the data of this small-scale model. The basis for estimating improvements in handling qualities from the type of data contained herein is undergoing further study.

A curve of static longitudinal stability parameter  $\partial C_m / \partial C_L$  versus wing tilt is presented in Figure 13. Pitching moment coefficient data are not presented because a defective balance gave erratic results. However, enough good pitching moment data were obtained to plot the curve of Figure 13. At wing tilts from  $10^\circ$  to  $45^\circ$ , the seaplane is very slightly stable. At higher wing tilts the parameter  $\partial C_m / \partial C_L$  goes strongly positive. However, this parameter becomes defective as an indicator of degree of stability at high wing tilts and low speeds. Differential thrust, envisioned as the hover and early transition control means, should provide adequate pitch control power to handle this "stability deficiency."

In view of the rapid drop-off of horsepower required through transition (Figure 8), extra installed horsepower is probably not required to accomplish this control. Note also that pitching moment coefficient was computed about a c.g. for hover with equal thrust loading on all six propellers. As the airplane passes through transition, the c.g. will move forward, due to weight shift of nacelles and wings. As stated in Reference 1, this c.g. shift should reduce instability by one-half.

An examination of Figure 10 shows that the seaplane is laterally and directionally stable at even the very highest wing tilts. Again,

however, the stability margin indicated is misleading at low speeds, and differential thrust and deflected thrust would probably be necessary for roll and yaw control and trim. Even with reduced vertical tail area, the seaplane still has adequate lateral-directional stability in transition.

Aerodynamics Laboratory  
David Taylor Model Basin  
Washington, D. C.  
October 1966

#### REFERENCES

1. Thomas, Richard O. Wind-Tunnel Investigation of a 1/20-Scale Powered Model Tilt-Wing V/STOL Seaplane in the Cruise Configuration. Wash., Aug 1965. 32 l. incl. illus. (David Taylor Model Basin. Rpt. 2079. Aero Rpt. 1093) (DDC AD 472 709)
2. Heyson, Harry H. Linearized Theory of Wind-Tunnel Jet-Boundary Corrections and Ground Effect for VTOL-STOL Aircraft. Wash., 1962. 269 p. incl. illus. (National Aeronautics and Space Administration. Tech. Rpt. R-124)
3. Jacobs, Eastman N. and Albert Sherman. Airfoil Section Characteristics as Affected by Variations of the Reynolds Number. Wash., 1937. 41 p. incl. illus. (National Advisory Committee for Aeronautics. Rpt. 586)
4. Perkins, Courtland D. and Robert E. Hage. Airplane Performance Stability and Control. N.Y., Wiley [1949]. 493 p. illus.
5. Hoerner, Sigward F. Fluid Dynamic Drag. [2d ed. Midland Park, N.J.] 1958. 1 v. illus.

Table 1  
Geometric and Physical Characteristics of a 1/20-Scale Powered  
Model Open-Ocean V/STOL Seaplane

Wing		
Section	NACA 4415	
Chord in feet		
Root	0.667	
Tip	0.333	
Taper Ratio	0.5	
Twist in degrees	0	
Aspect Ratio	10	
Mean geometric chord in feet	0.518	
Span in feet	5.0	
Area in square feet	2.5	
Development line (percent chord)	25	
Canard		
Section	NACA 4415	
Chord in feet		
Root	0.333	
Tip	0.167	
Taper Ratio	0.5	
Twist in degrees	0	
Aspect Ratio	10	
Mean geometric chord in feet	0.259	
Span in feet	2.5	
Area in square feet	0.625	
Development line (percent chord)	25	
Vertical Tail		
Section		
Root	NACA 0012	
Tip	NACA 0009	
Chord in feet		
Root	0.850	
Tip	0.546	

Table 1 (Concluded)

Vertical Tail (Concluded)

Taper Ratio	0.643
Mean geometric chord in feet	0.708
Span in feet	1.216
Area in square feet (excluding dorsal fin)	0.848
Sweep of quarter chord line in degrees	24.5
Area of dorsal fin in square feet	0.105

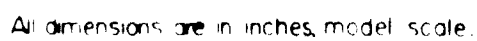
Propellers (All)

Diameter in feet	1.0
------------------	-----

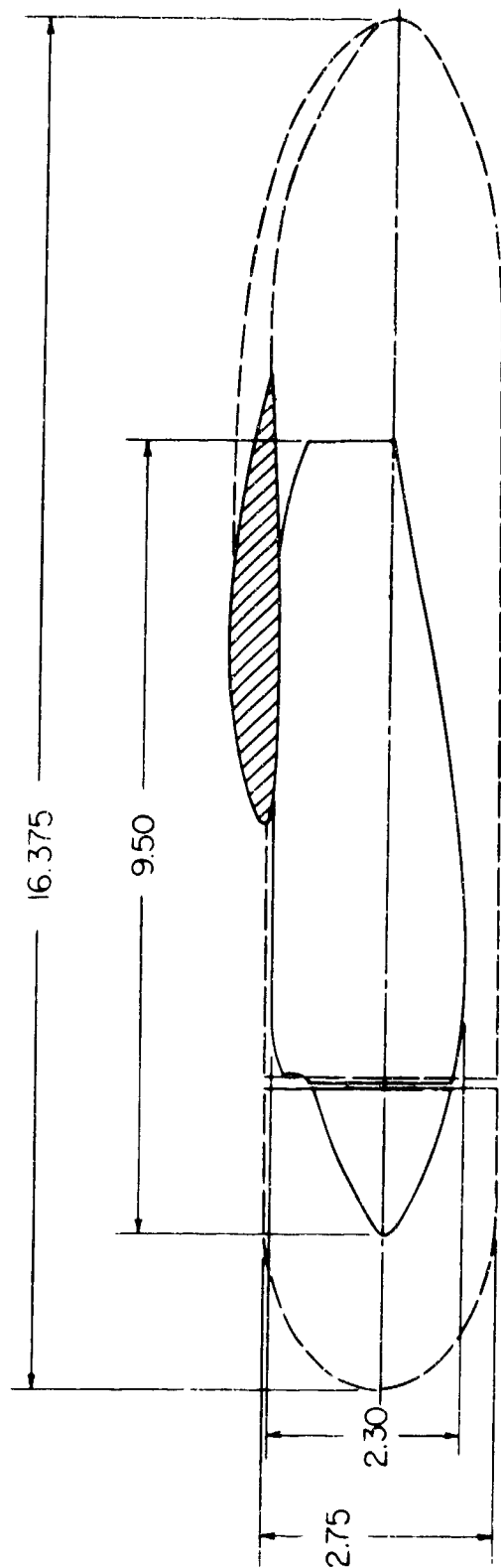
Table 2

Summary of Wind Tunnel Test Conditions for a 1/20-Scale Powered  
Model V/STOL Seaplane in the Transition Configuration

Spoilers	Wing Incidence in deg	q in lb/ft <sup>2</sup>	V in knots	Reynolds Number per foot $\times 10^{-6}$
Off	10	4.0	35.5	4.96
	20	4.0	35.5	4.96
	40	4.65	38.3	5.36
	50	4.27	36.7	5.13
	60	2.96	30.5	4.26
	70	0.95	17.3	2.41
	80	0.13	6.3	0.884
	90	0	0	0
On	10	4.0	35.5	4.96
	20	4.0	35.5	4.96
	30	4.0	35.5	4.96
	40	4.0	35.5	4.96
	50	4.27	36.7	5.13
	60	2.96	17.3	4.26
	70	0.95	17.3	2.41
	80	0.13	6.34	0.884



### (a) Three-View Drawing



All dimensions are in inches, model scale.

Figure 1 (Concluded)

(b) Relative Sizes of the Motor Nacelle and the Scale Nacelle

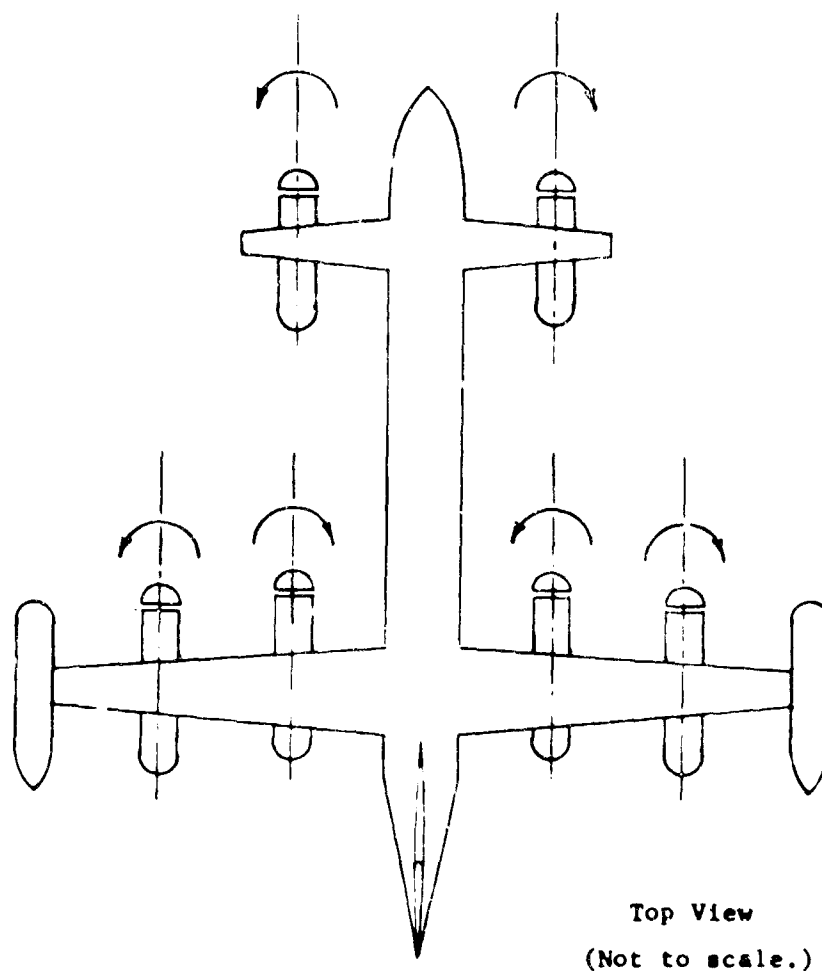


Figure 2 - Propeller Rotation Directions for a 1/20-Scale  
Powered Model V/STOL Seaplane



Figure 3 - Photographs of the Seaplane Model in the Wind Tunnel  
(a) Wing Tilt,  $0^\circ$

PSD-316,355



Figure 3 (Continued)  
(b) Wing Tilt,  $45^\circ$

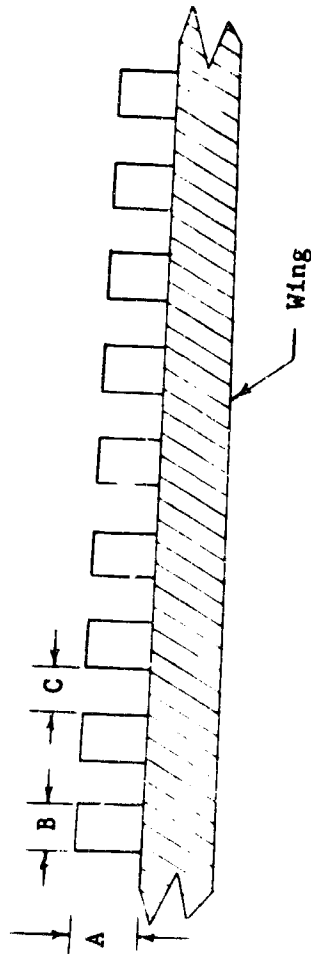
PSD-316,353



Figure 3 (Concluded)  
(c) Wing Tilt,  $90^\circ$

PSD-316,356

Dimensions	
A	height = $0.10\ c$
B	width = $0.06\ c$
C	gap = $0.06\ c$



Note: Spoilers are located at 15 percent local chord.

Figure 4 - Dimensions of Full-Span Spoilers for Wing and Canard  
of 1/20-Scale V/STOL Seaplane Model

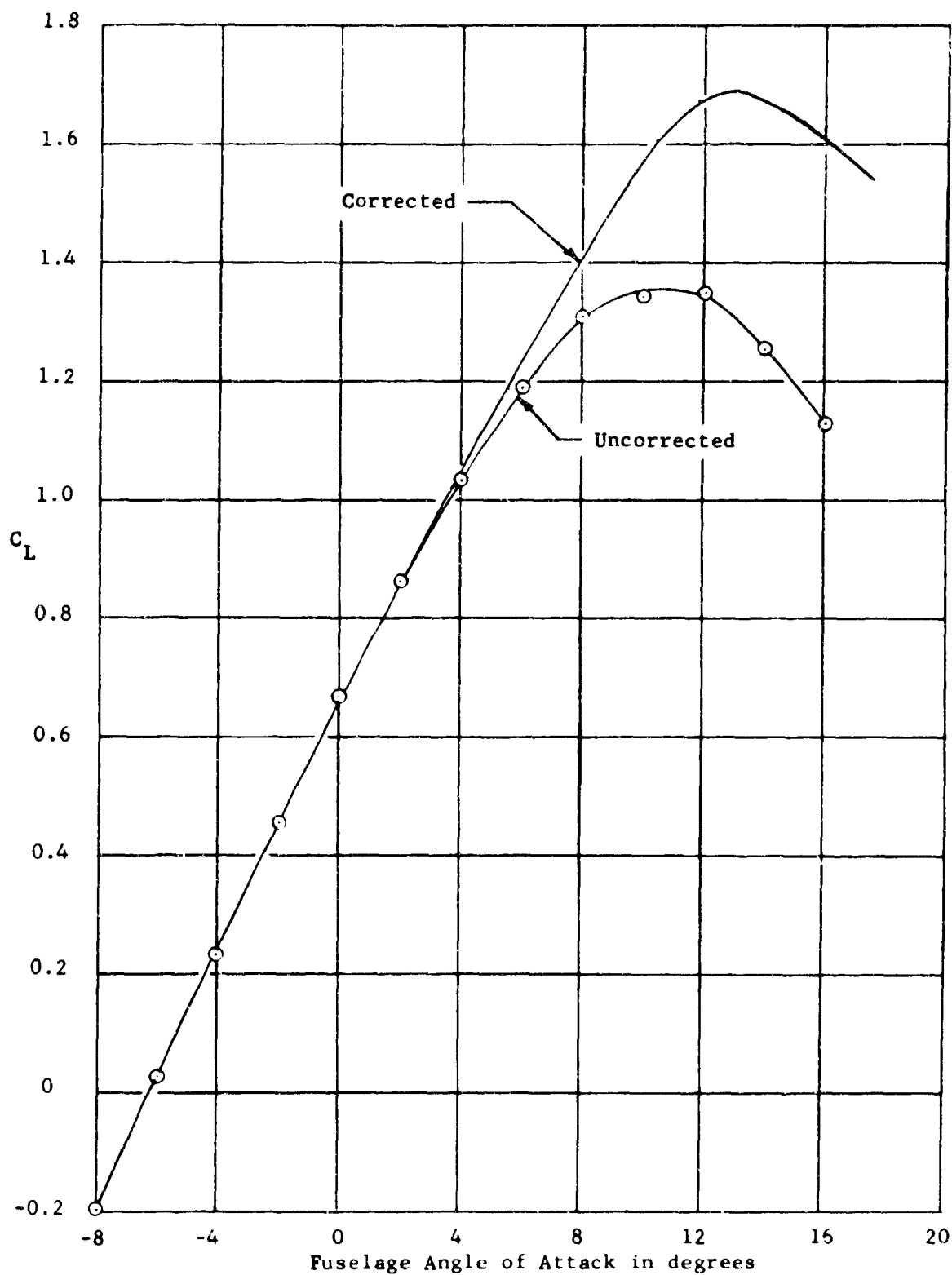


Figure 5 - Effect of Reynolds Number Correction to Minimum Drag and  $C_{L_{max}}$  on Aerodynamic Characteristics of Open-Ocean V/STOL Seaplane

(a)  $C_L$  Versus  $\alpha$

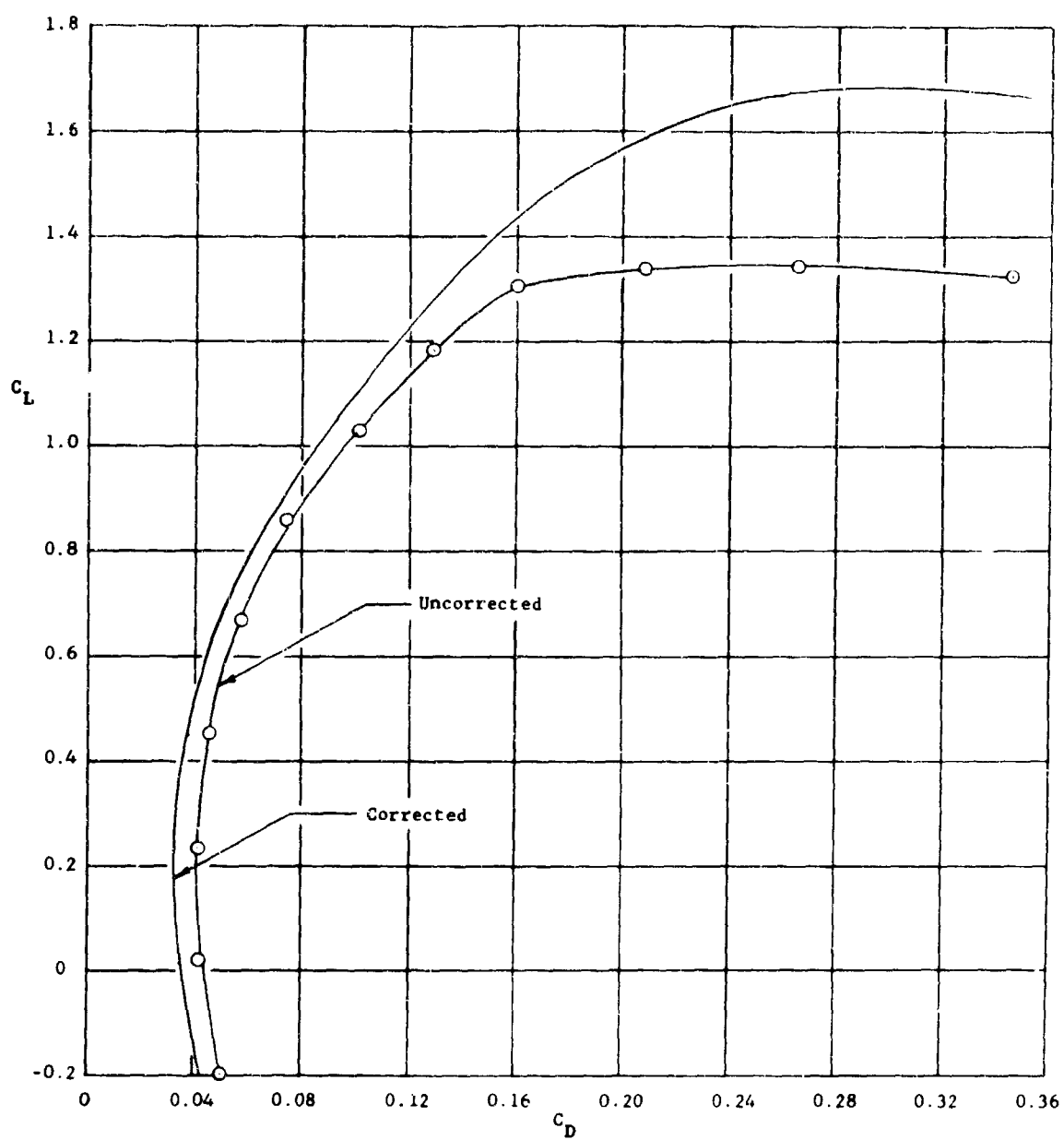


Figure 5 (Continued)

(b) Drag Polar

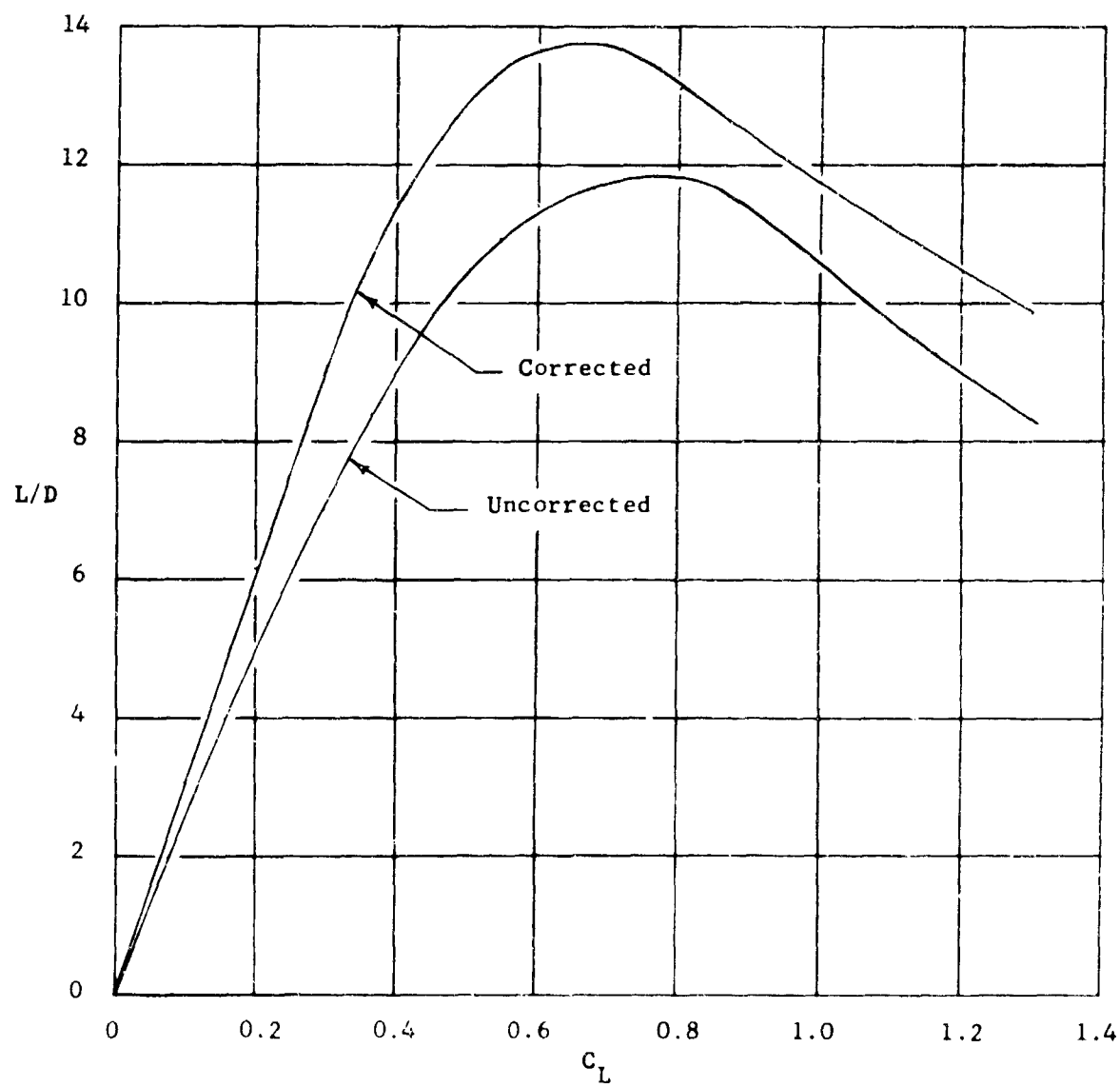


Figure 5 (Concluded)  
(c) Lift-Drag Ratio

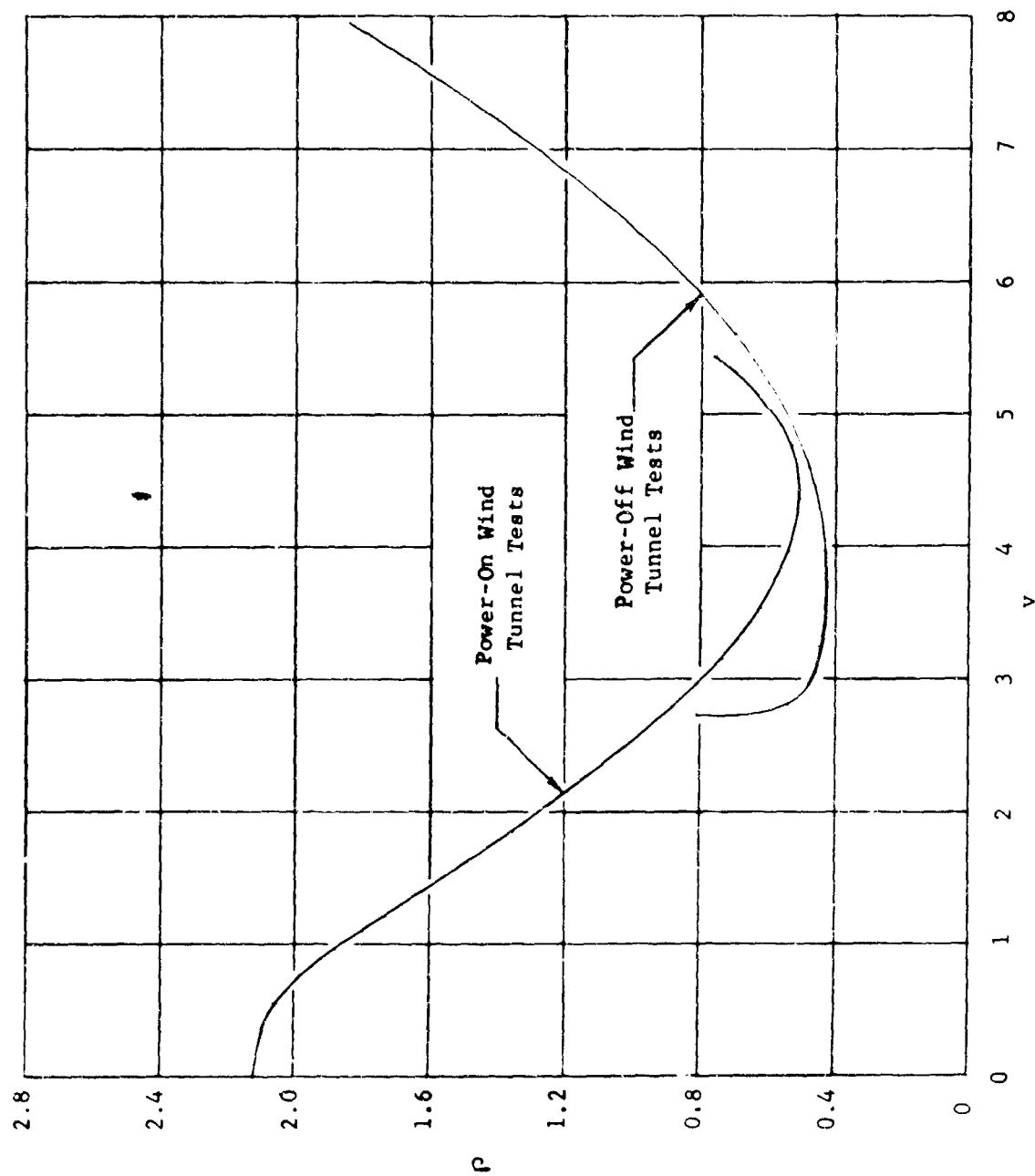


Figure 6 - Power Required Parameter as Measured in the Wind Tunnel and Calculated From Power-Off Wind Tunnel Tests

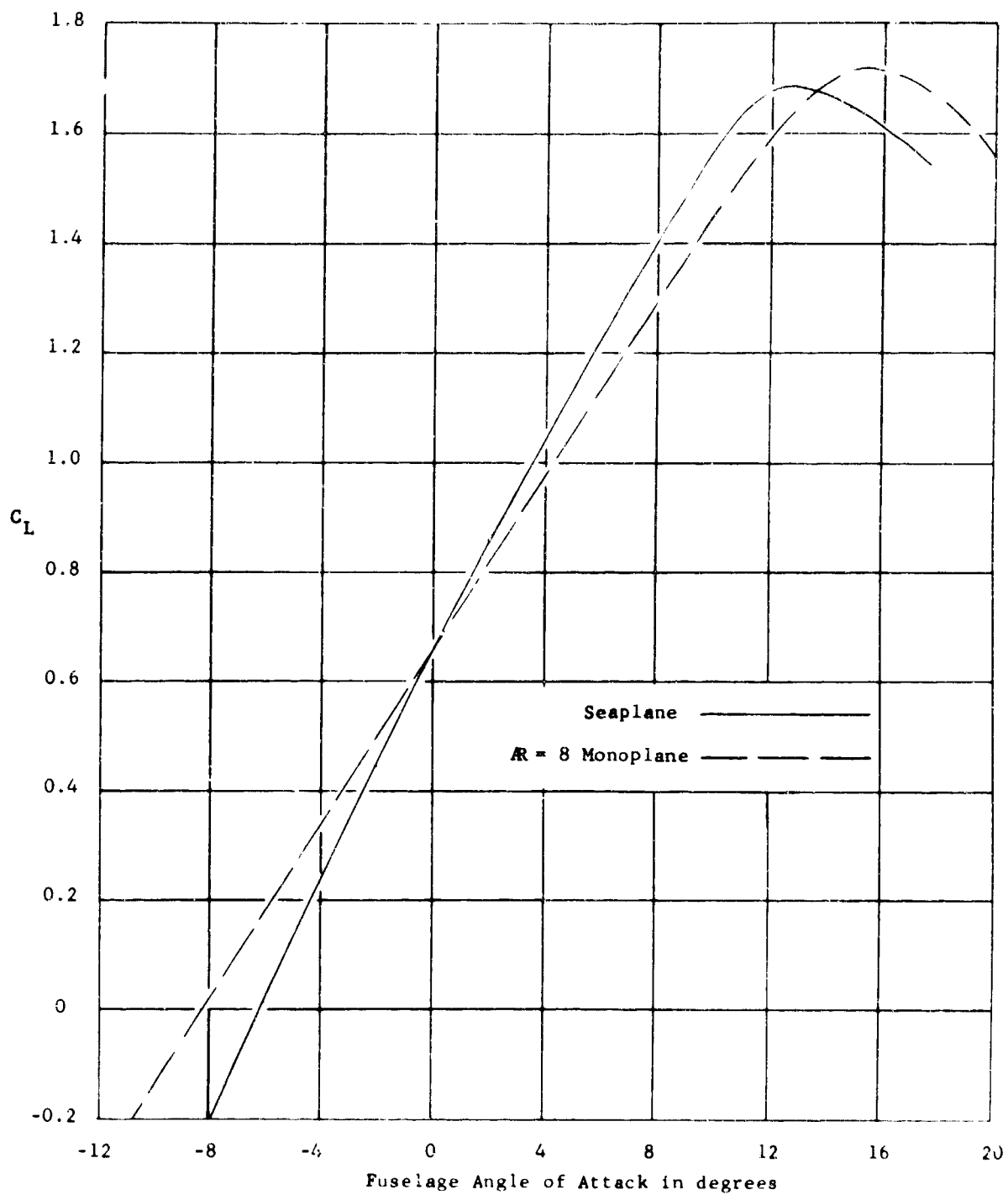


Figure 7 - Performance Comparison of the Seaplane With a Monoplane  
of Equivalent Size and Aspect Ratio

(a)  $C_L$  Versus  $\alpha$

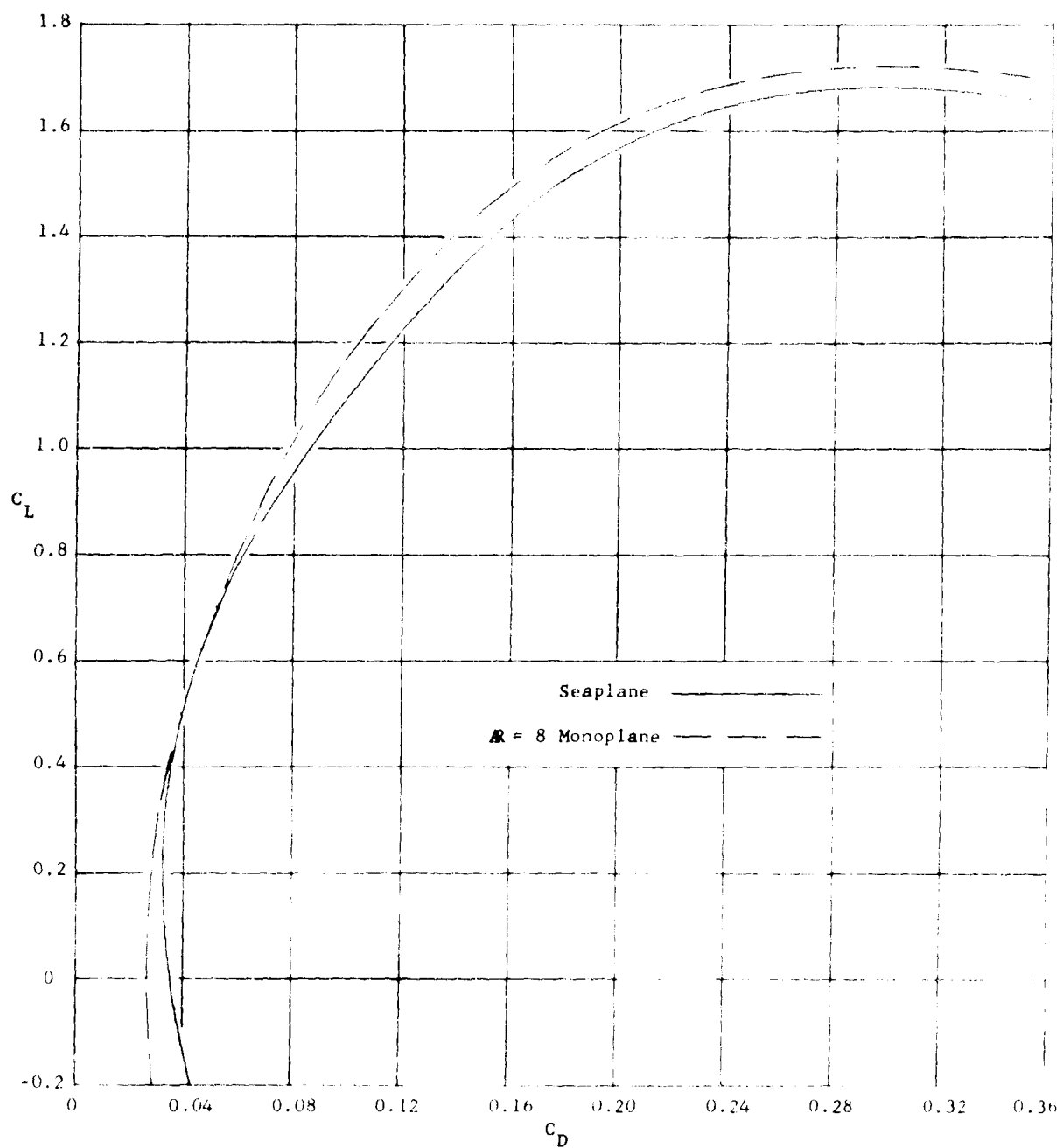


Figure 7 (Continued)  
(b) Drag Polar

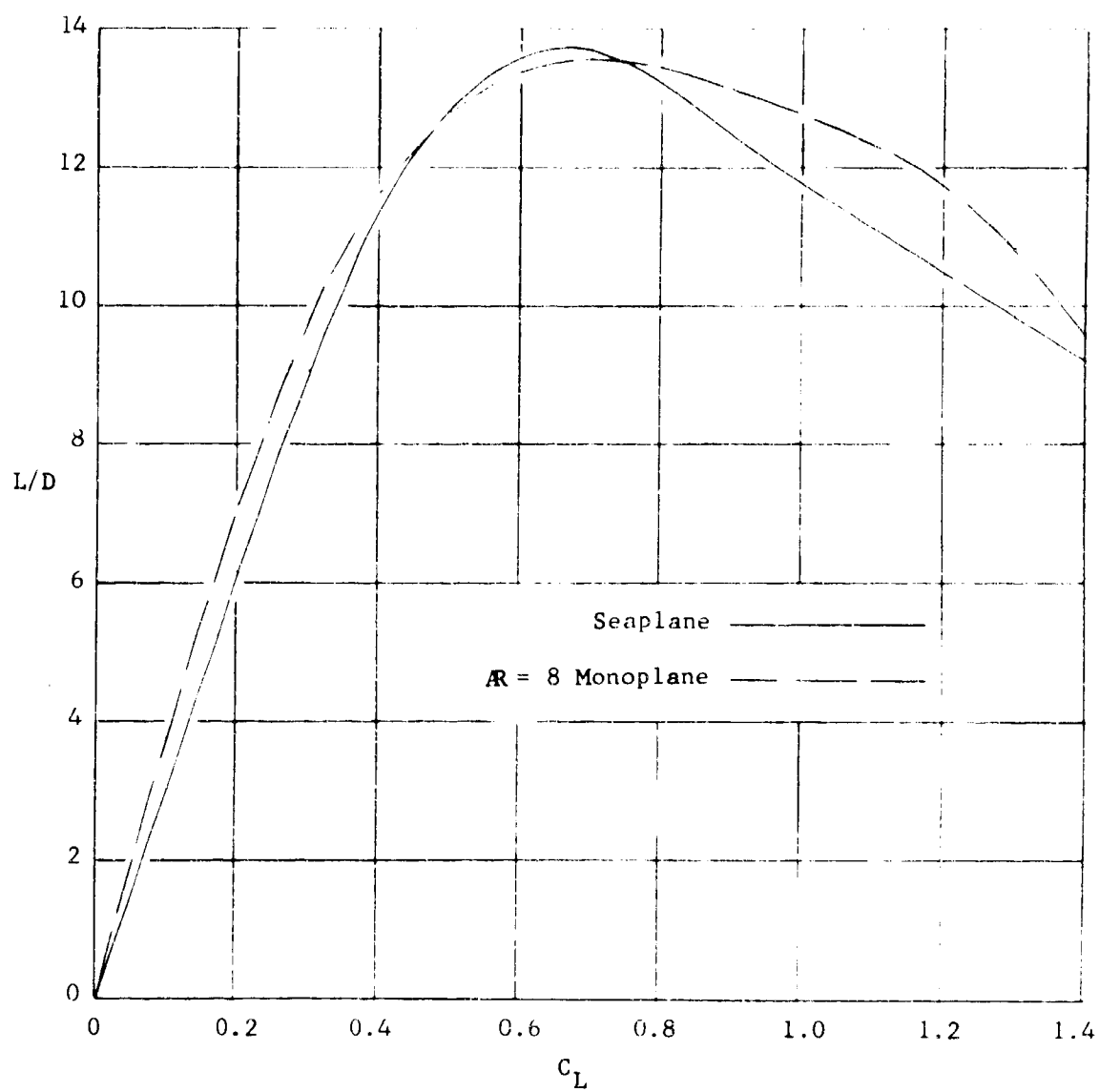


Figure 7 (Continued)  
(c) Lift-Drag Ratio

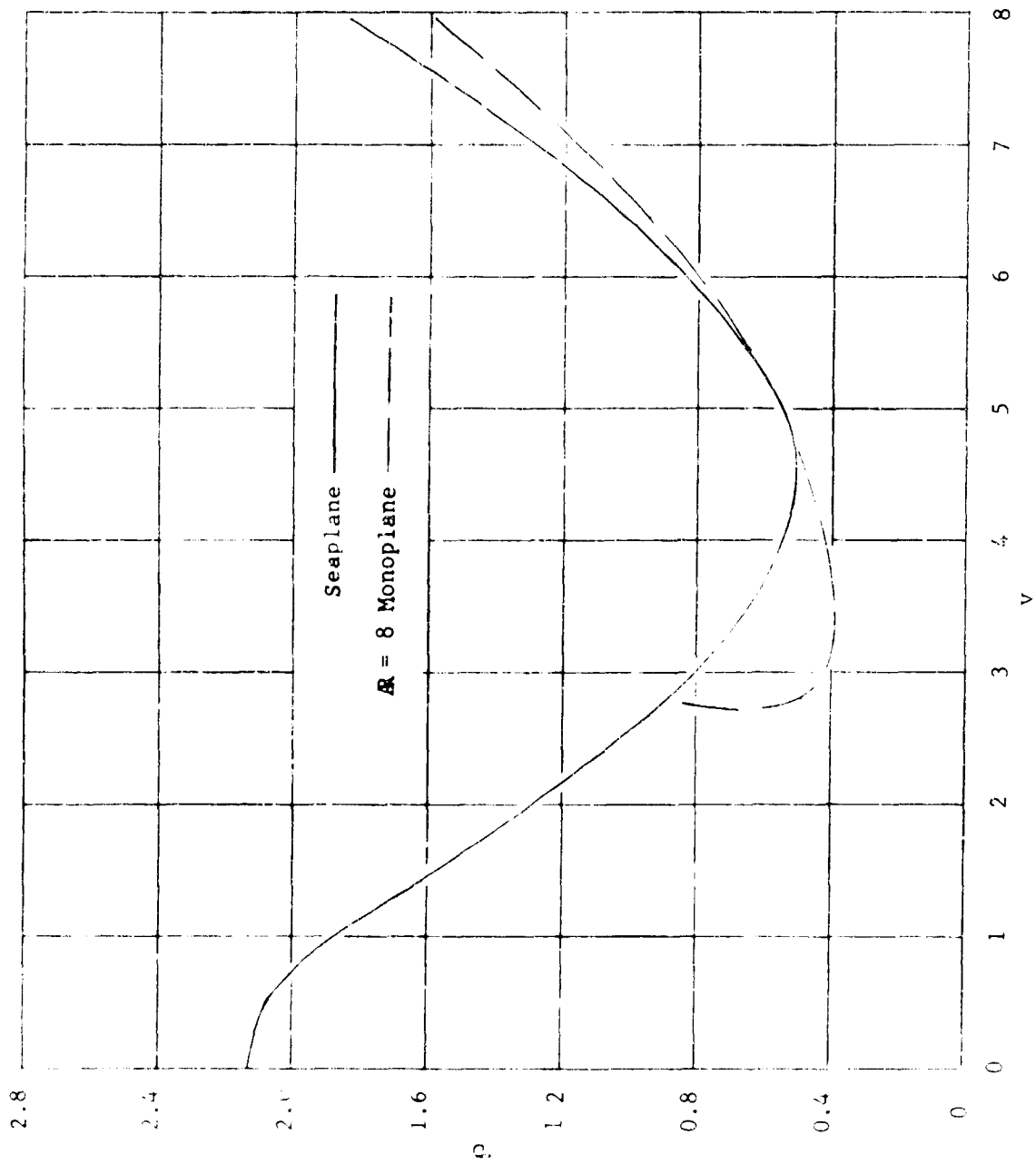


Figure 7 (Concluded)

(d) Power Required Parameter Versus Speed Parameter

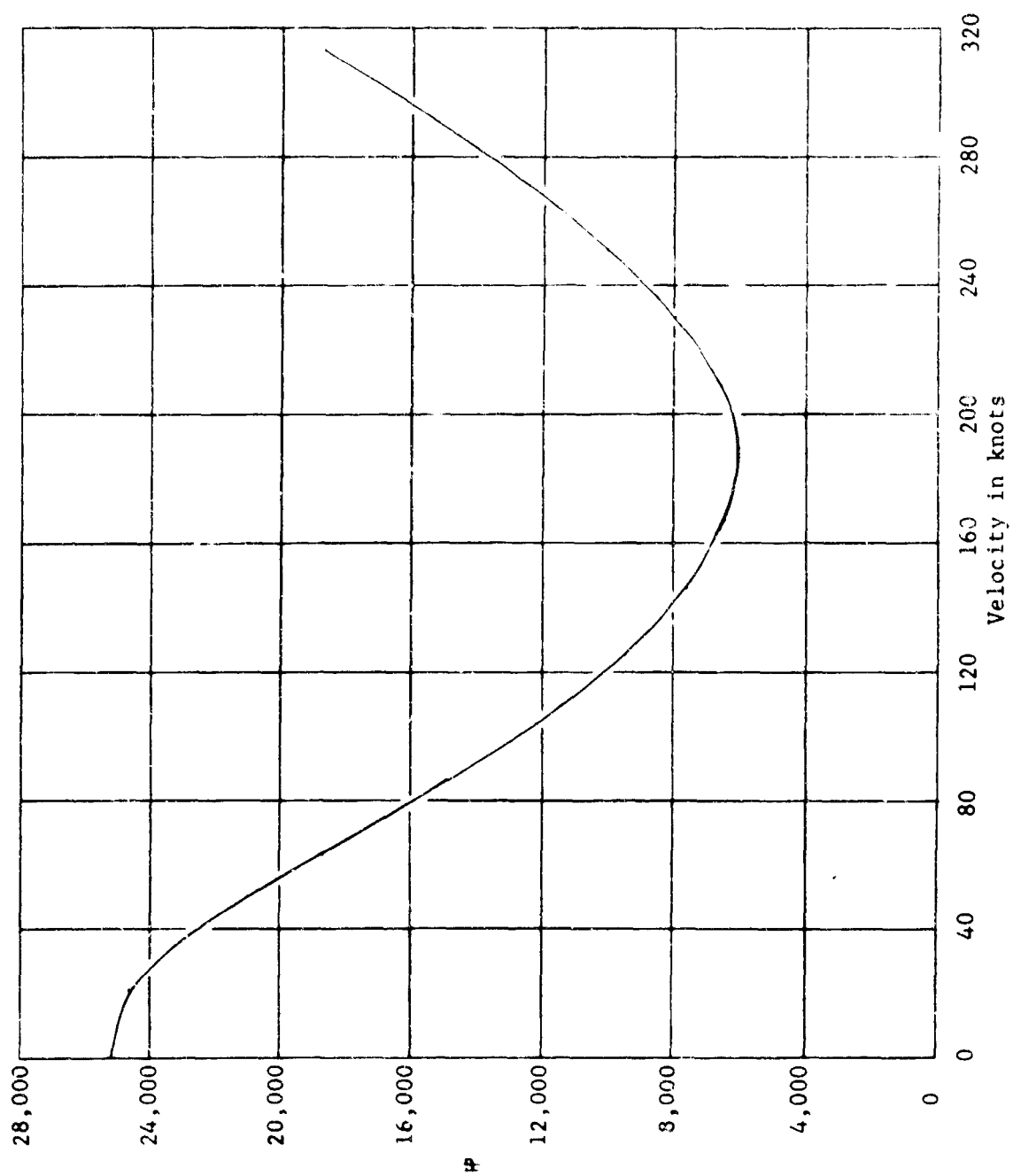


Figure 8 - Horsepower Required Versus Speed for a Full-Scale Seaplane.

Sea Level; Standard Day; Weight = 90,000 Pounds

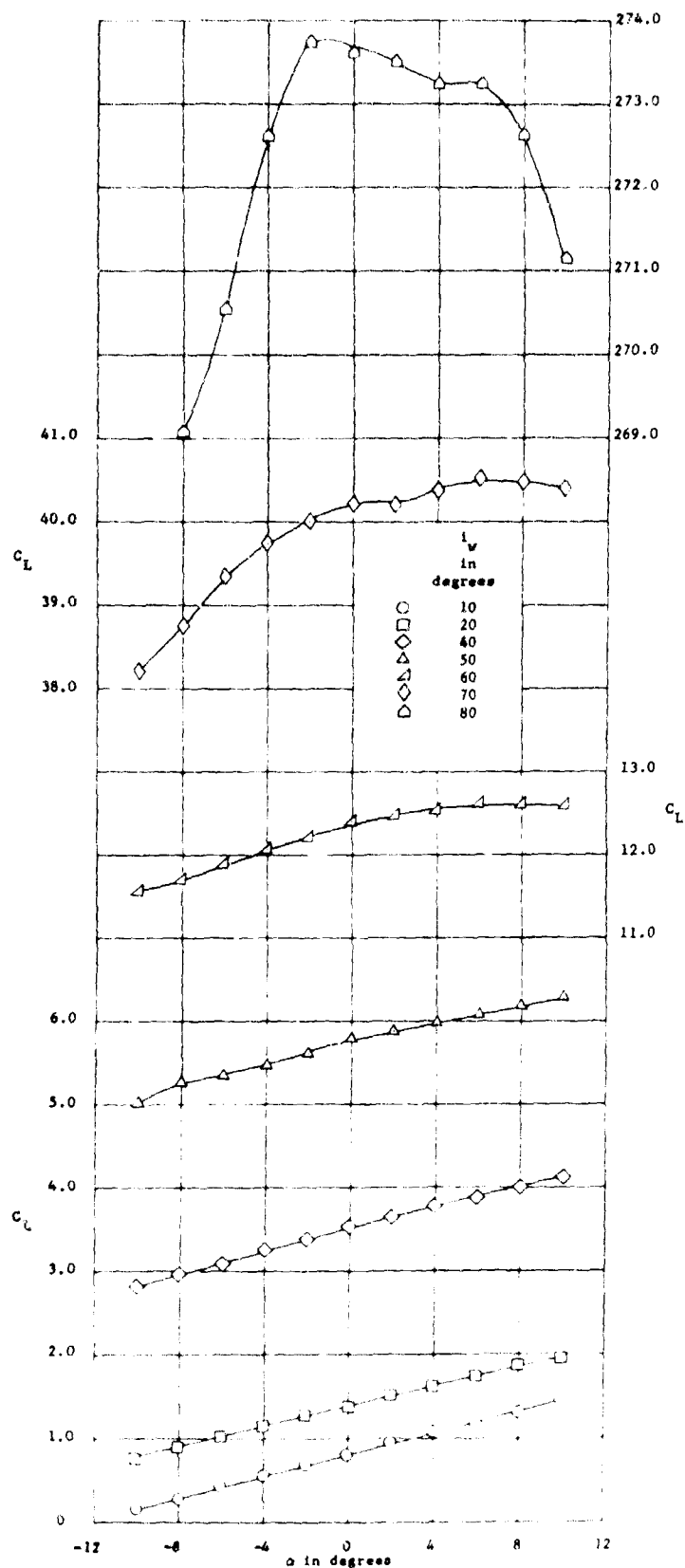


Figure 9 - Longitudinal Aerodynamic Characteristics in Pitch at Various Wing Tilts for a 1/20-Scale Model V/STOL Seaplane. Thrust Set for  $C_D = 0$  at  $\alpha = 0^\circ$   
 (a)  $C_L$  Versus  $\alpha$

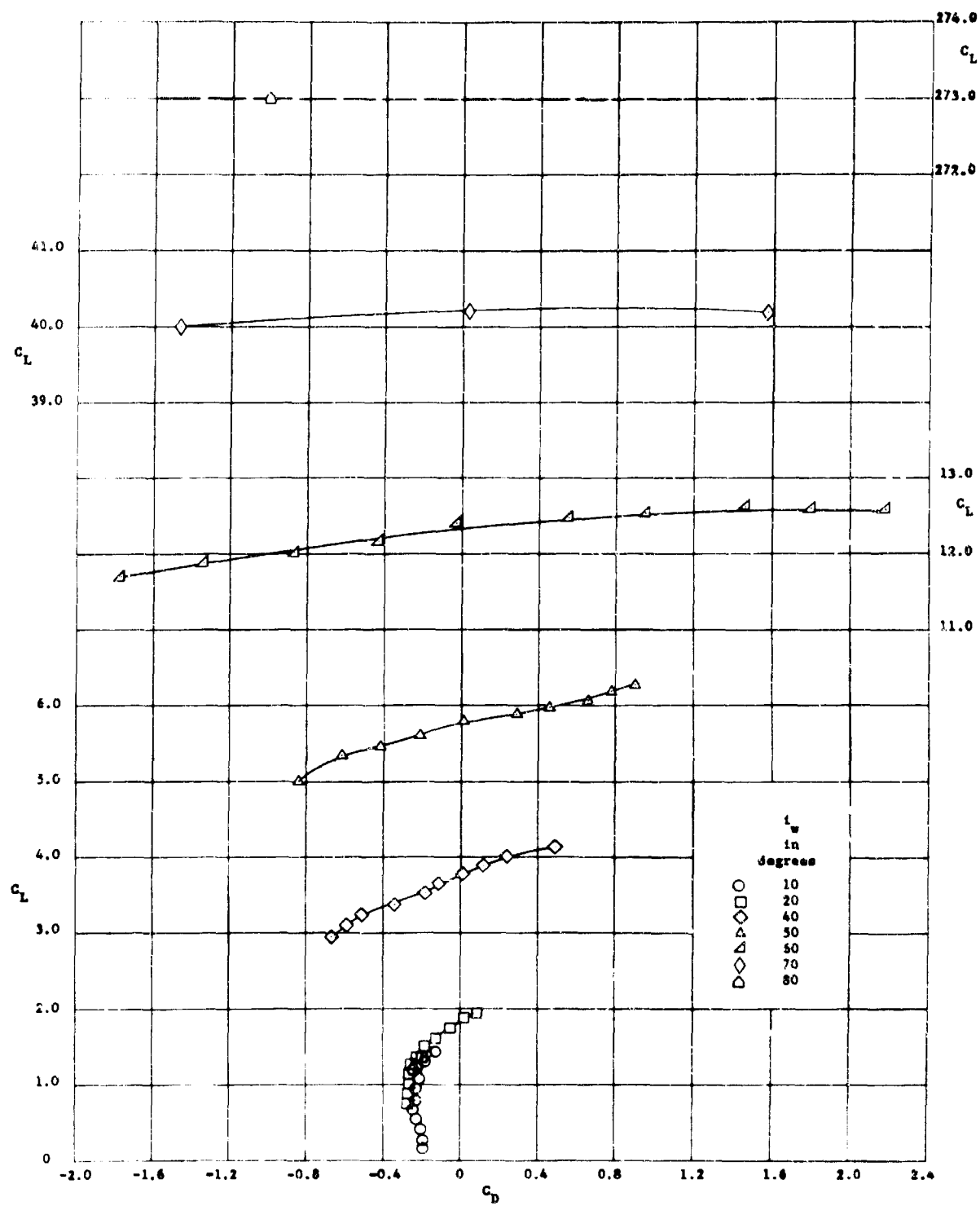


Figure 9 (Concluded)  
(b)  $C_L$  Versus  $C_D$

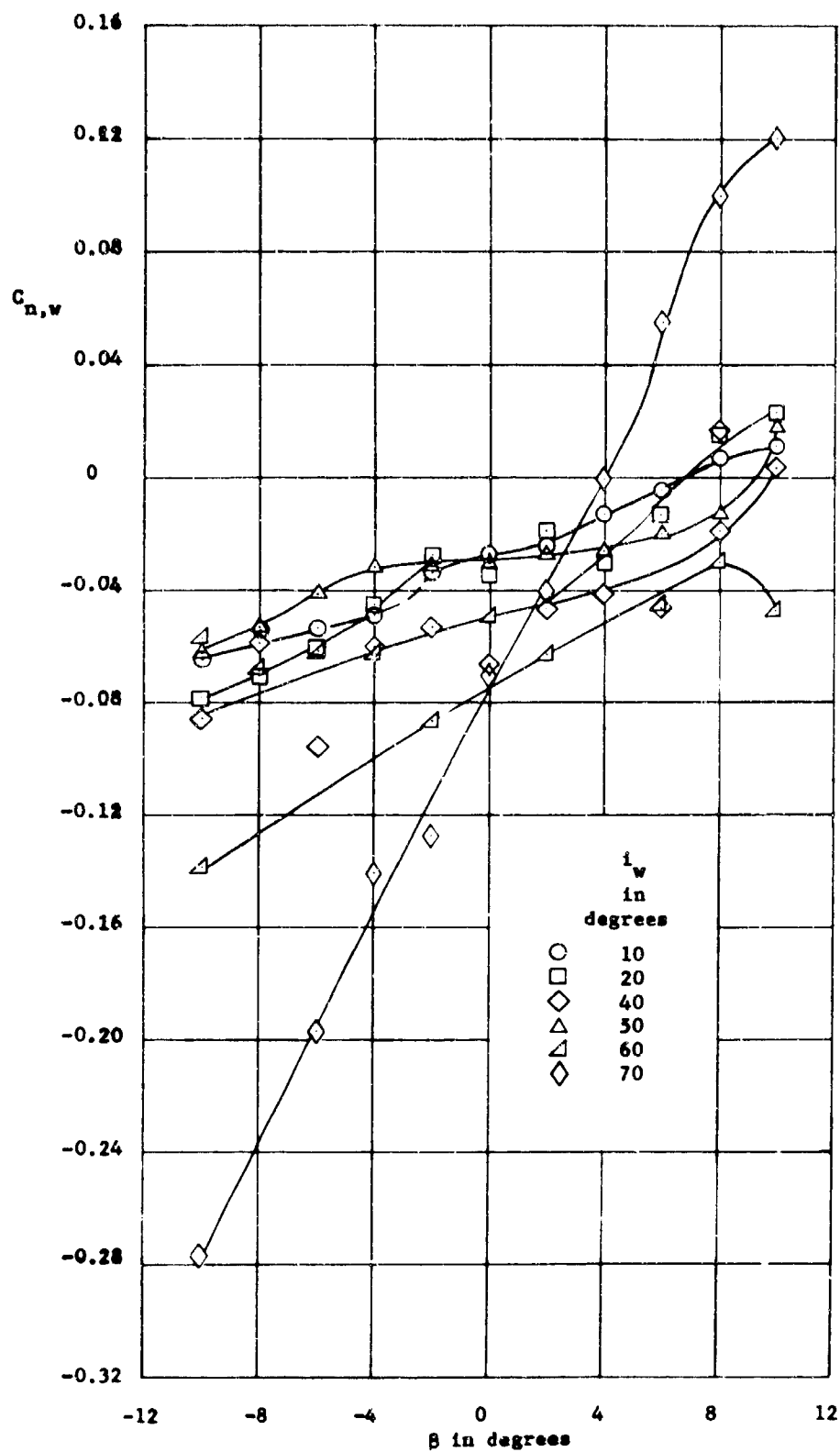


Figure 10 - Lateral-Directional Aerodynamic Characteristics in Sideslip  
at Various Wing Tilts for a 1/20-Scale Model V/STOL Seaplane.

Thrust Set for  $C_D = 0$  at  $\alpha = 0^\circ$

(a) Yawing Moment

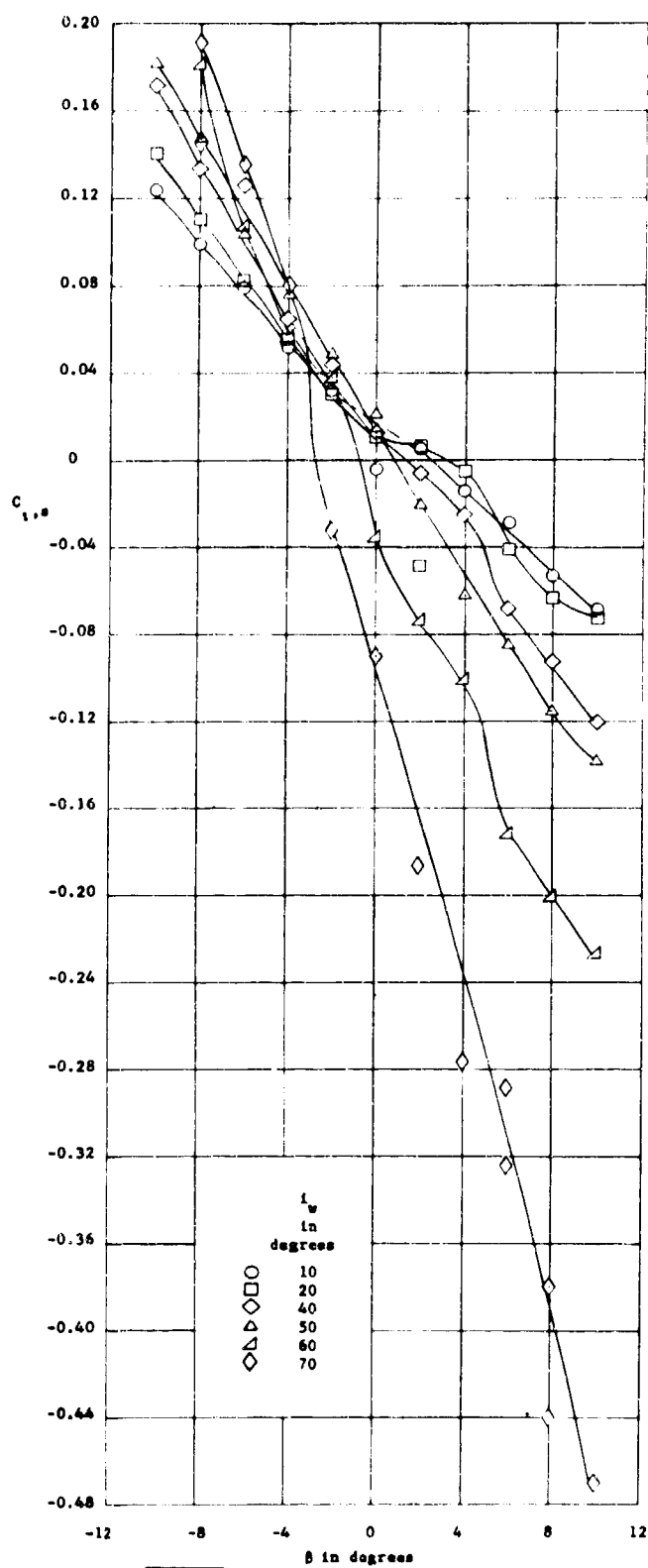


Figure 10 (Continued)

(b) Rolling Moment

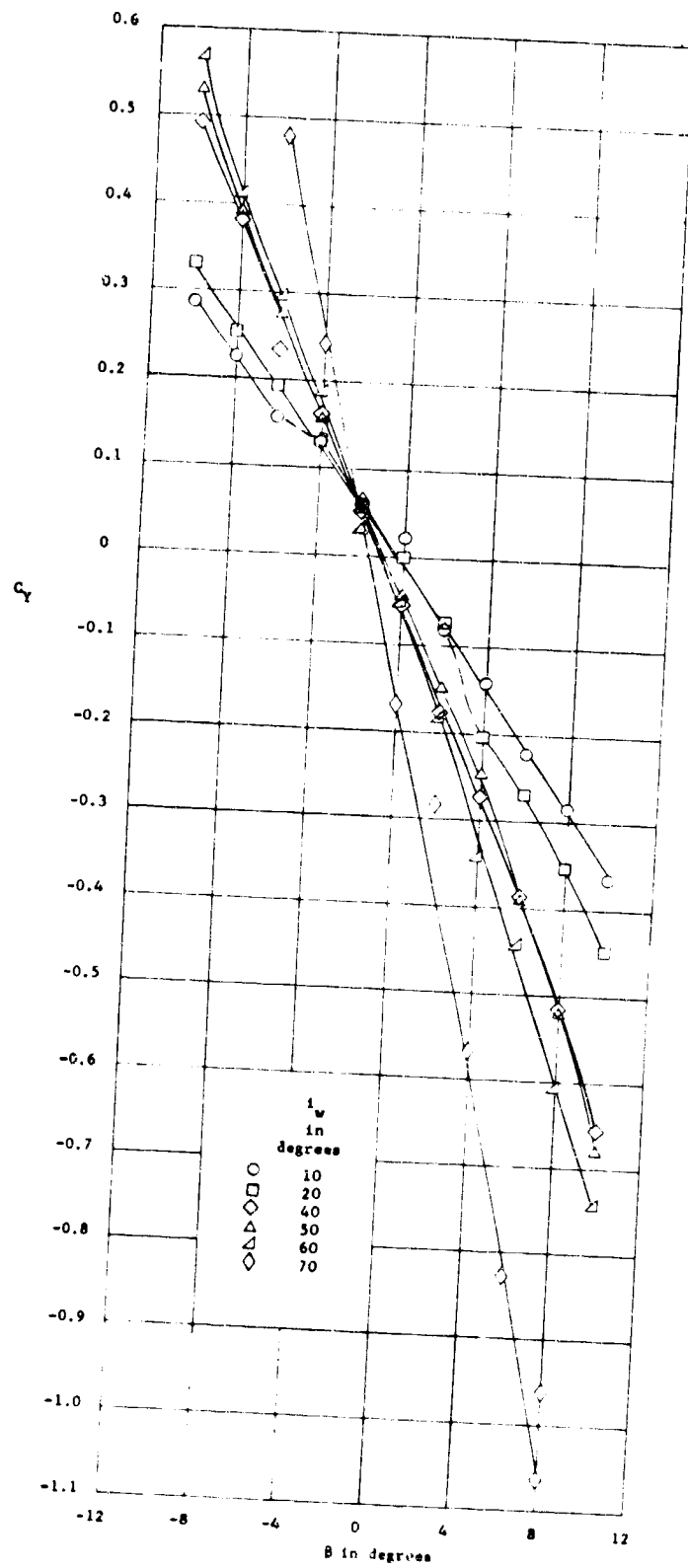


Figure 10 (Concluded)

(c) Side Force

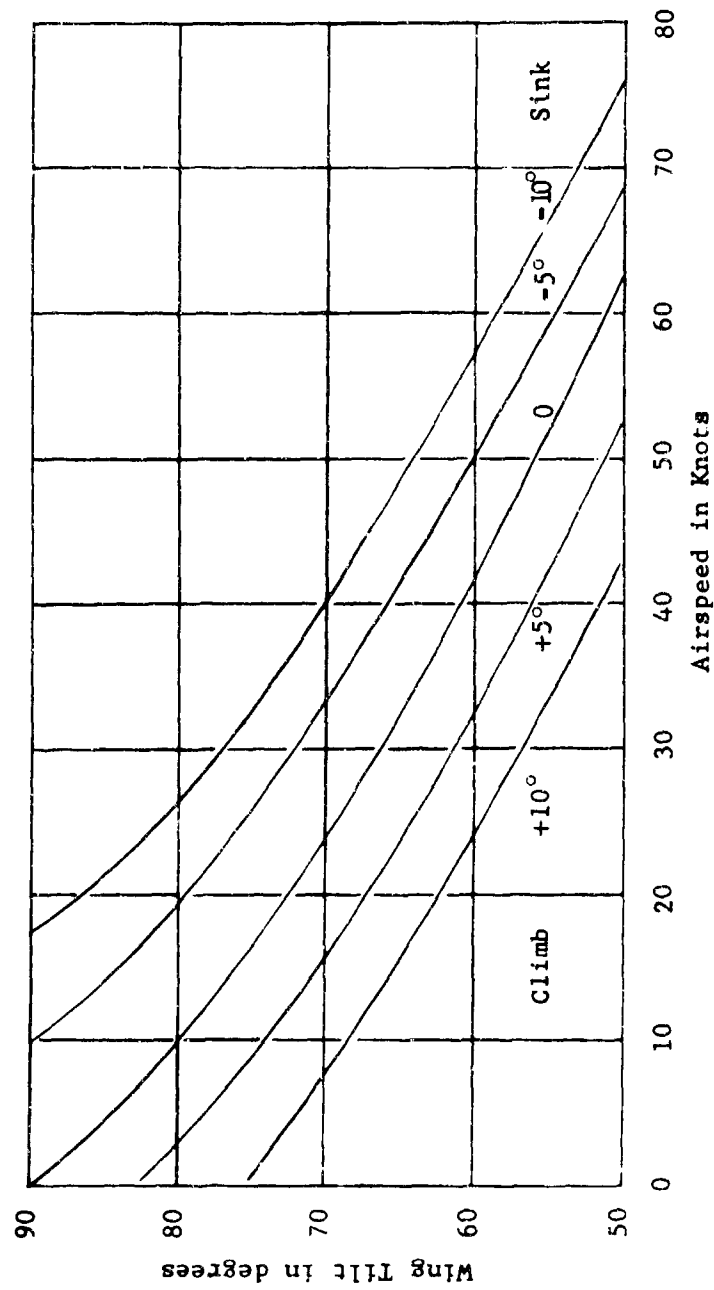


Figure 11 - Wing Tilt Versus Airspeed for Various Climb and Sink Angles. Fuselage Level; Spoilers Off; Weight = 93,000 Pounds; Sea Level, Standard Day

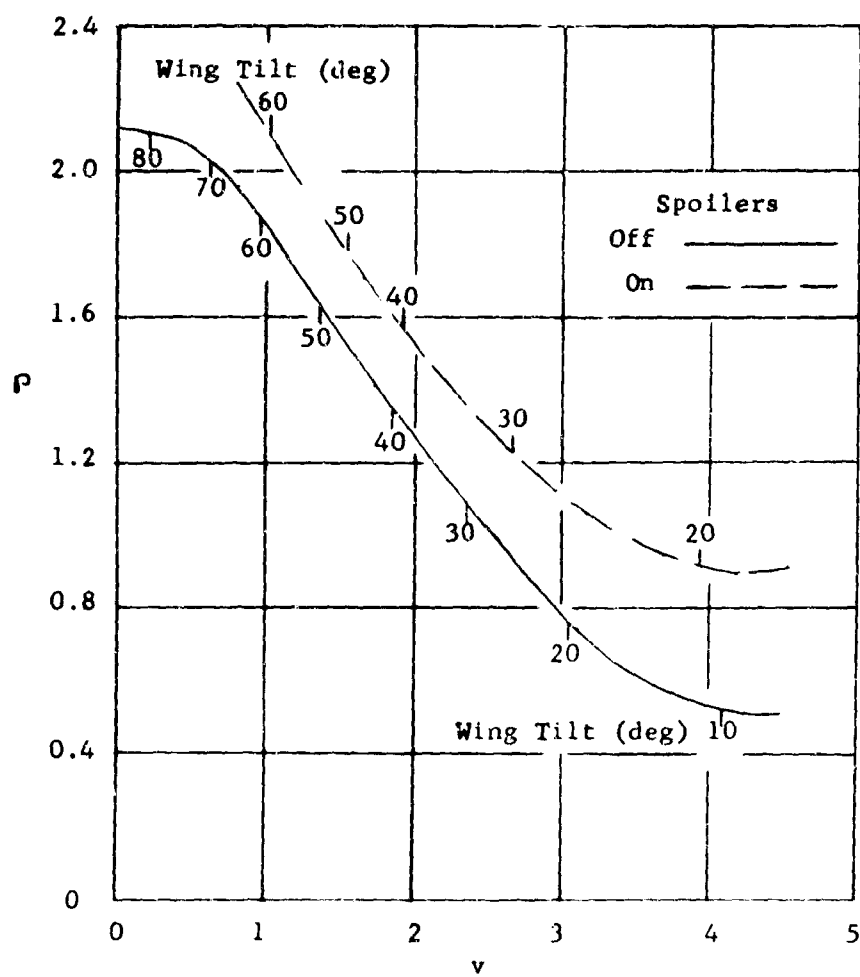


Figure 12 - Effect of Full-Span Spoilers  
on Power Required

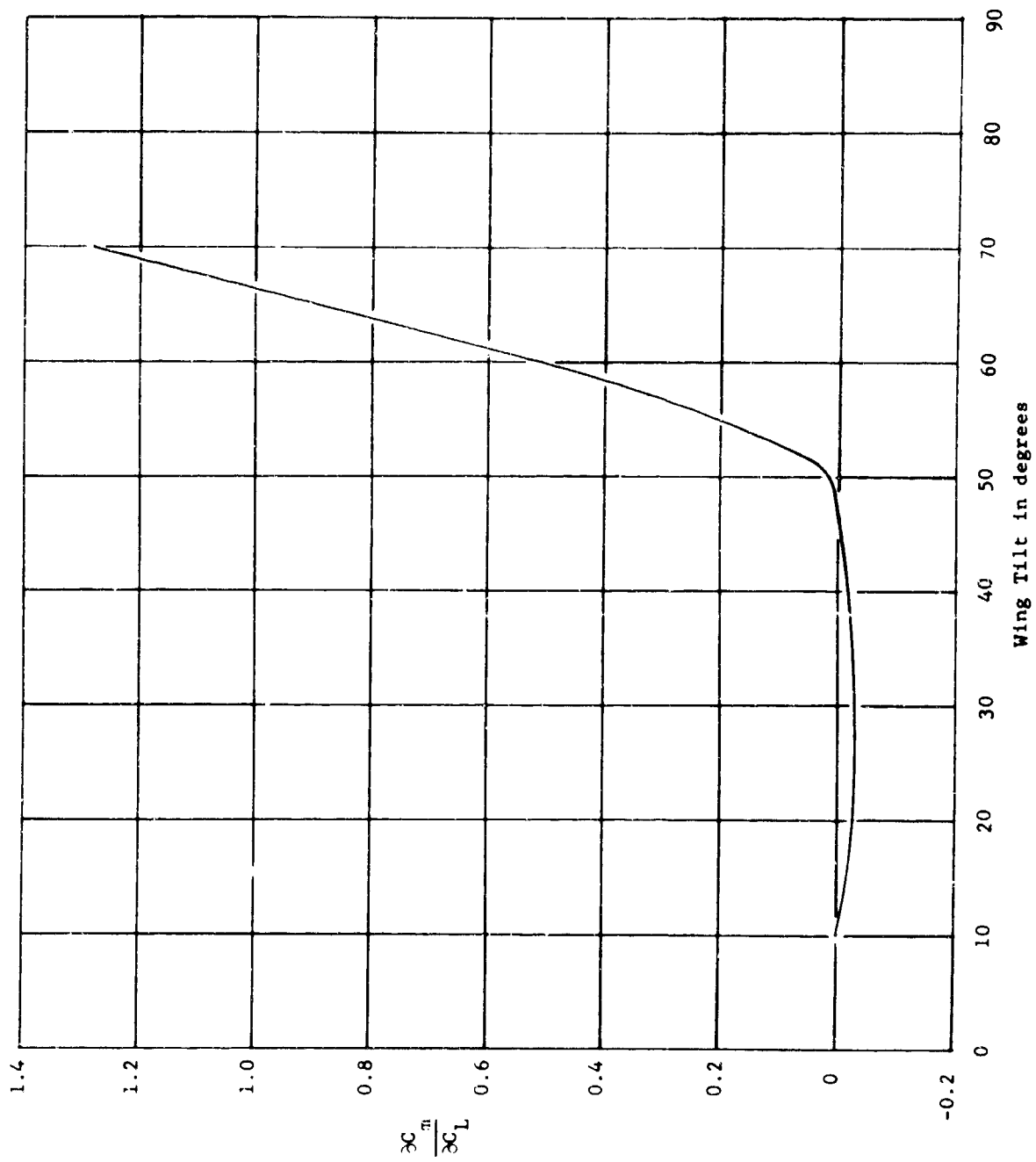


Figure 13 - Static Longitudinal Stability Versus Wing Tilt

Unclassified

Security Classification

DOCUMENT CONTROL DATA - R&D		
<small>(Security classification of title, body of abstract and indexing annotation must be entered when the overall report is classified)</small>		
1. ORIGINATING ACTIVITY (Corporate author) Aerodynamics Laboratory David Taylor Model Basin Washington, D. C. 20007		2a. REPORT SECURITY CLASSIFICATION Unclassified
		2b. GROUP
3. REPORT TITLE SUMMARY REPORT OF WIND-TUNNEL INVESTIGATIONS OF A 1/20-SCALE POWERED MODEL OPEN-OCEAN V/STOL SEAPLANE		
4. DESCRIPTIVE NOTES (Type of report and inclusive dates)		
5. AUTHOR(S) (Last name, first name, initial) Thomas, Richard O.		
6. REPORT DATE January 1967	7a. TOTAL NO. OF PAGES 38[6]	7b. NO. OF REFS 5
8a. CONTRACT OR GRANT NO. WF 012 01 06	8b. ORIGINATOR'S REPORT NUMBER(S) Report 2181	
a. PROJECT NO.		
c.	8c. OTHER REPORT NO(S) (Any other numbers that may be assigned this report) Aero Report 1106	
d. Aero Problem 632-556		
10. AVAILABILITY/LIMITATION NOTICES Distribution of this document is unlimited.		
11. SUPPLEMENTARY NOTES	12. SPONSORING MILITARY ACTIVITY Naval Air Systems Command Department of the Navy Washington, D. C. 20360	
13. ABSTRACT Low-speed wind-tunnel tests were conducted on a 1/20-scale powered model of a proposed open-ocean V/STOL seaplane design. Hover and transition power required and climb and descent speeds at various flight path angles were determined. The effect of full-span spoilers on wing and canard stalling characteristics through transition was briefly investigated.  A comparison of cruise performance of the seaplane and a conventional transport of equivalent size was made. After correction of the seaplane model cruise lift curve and drag polar to full-scale Reynolds number, cruise performance of the seaplane was found to compare favorably with that of the conventional monoplane.  In the transition mode, the model is longitudinally unstable at high wing tilts and directionally at all wing tilts for the initial center-of-gravity location. With the present relationship of wing, canard, and center of gravity, the model cannot be trimmed in pitch by varying only incidence of the canard with uniform thrust setting on all engines. Differential thrust, the mechanism envisioned for hover control, is necessary for pitch trim and control throughout most of the transition mode.		

DD FORM 1473  
1 JAN 64

Unclassified

Security Classification

Unclassified  
Security Classification

14 KEY WORDS	LINK A		LINK B		LINK C	
	ROLE	WT	ROLE	WT	ROLE	WT
V/STOL Aircraft Transition Flight Hovering Flight Tandem Tilt-Wing V/STOL Aircraft Powered Seaplane Model Seaplane Antisubmarine Aircraft Longitudinal Stability Lateral Stability STOL Performance Canard						

#### INSTRUCTIONS

1. **ORIGINATING ACTIVITY:** Enter the name and address of the contractor, subcontractor, grantee, Department of Defense activity or other organization (*corporate author*) issuing the report.

2a. **REPORT SECURITY CLASSIFICATION:** Enter the overall security classification of the report. Indicate whether "Restricted Data" is included. Marking is to be in accordance with appropriate security regulations.

2b. **GROUP:** Automatic downgrading is specified in DoD Directive 5200.10 and Armed Forces Industrial Manual. Enter the group number. Also, when applicable, show that optional markings have been used for Group 3 and Group 4 as authorized.

3. **REPORT TITLE:** Enter the complete report title in all capital letters. Titles in all cases should be unclassified. If a meaningful title cannot be selected without classification, show title classification in all capitals in parenthesis immediately following the title.

4. **DESCRIPTIVE NOTES:** If appropriate, enter the type of report, e.g., interim, progress, summary, annual, or final. Give the inclusive dates when a specific reporting period is covered.

5. **AUTHOR(S):** Enter the name(s) of author(s) as shown on or in the report. Enter last name, first name, middle initial. If military, show rank and branch of service. The name of the principal author is an absolute minimum requirement.

6. **REPORT DATE:** Enter the date of the report as day, month, year, or month, year. If more than one date appears on the report, use date of publication.

7a. **TOTAL NUMBER OF PAGES:** The total page count should follow normal pagination procedures, i.e., enter the number of pages containing information.

7b. **NUMBER OF REFERENCES:** Enter the total number of references cited in the report.

8a. **CONTRACT OR GRANT NUMBER:** If appropriate, enter the applicable number of the contract or grant under which the report was written.

8b, 8c, & 8d. **PROJECT NUMBER:** Enter the appropriate military department identification, such as project number, subproject number, system numbers, task number, etc.

9a. **ORIGINATOR'S REPORT NUMBER(S):** Enter the official report number by which the document will be identified and controlled by the originating activity. This number must be unique to this report.

9b. **OTHER REPORT NUMBER(S):** If the report has been assigned any other report numbers (*either by the originator or by the sponsor*), also enter this number(s).

10. **AVAILABILITY/LIMITATION NOTICES:** Enter any limitations on further dissemination of the report, other than those

imposed by security classification, using standard statements such as:

- (1) "Qualified requesters may obtain copies of this report from DDC."
- (2) "Foreign announcement and dissemination of this report by DDC is not authorized."
- (3) "U. S. Government agencies may obtain copies of this report directly from DDC. Other qualified DDC users shall request through \_\_\_\_\_."
- (4) "U. S. military agencies may obtain copies of this report directly from DDC. Other qualified users shall request through \_\_\_\_\_."
- (5) "All distribution of this report is controlled. Qualified DDC users shall request through \_\_\_\_\_."

If the report has been furnished to the Office of Technical Services, Department of Commerce, for sale to the public, indicate this fact and enter the price, if known.

11. **SUPPLEMENTARY NOTES:** Use for additional explanatory notes.

12. **SPONSORING MILITARY ACTIVITY:** Enter the name of the departmental project office or laboratory sponsoring (paying for) the research and development. Include address.

13. **ABSTRACT:** Enter an abstract giving a brief and factual summary of the document indicative of the report, even though it may also appear elsewhere in the body of the technical report. If additional space is required, a continuation sheet shall be attached.

It is highly desirable that the abstract of classified reports be unclassified. Each paragraph of the abstract shall end with an indication of the military security classification of the information in the paragraph, represented as (TS) (S) (C) or (U).

There is no limitation on the length of the abstract. However, the suggested length is from 150 to 225 words.

14. **KEY WORDS:** Key words are technically meaningful terms or short phrases that characterize a report and may be used as index entries for cataloging the report. Key words must be selected so that no security classification is required. Identifiers, such as equipment model designation, trade name, military project code name, geographic location, may be used as key words but will be followed by an indication of technical content. The assignment of links, roles, and weights is optional.

Unclassified  
Security Classification